Glycobiology, 2018, vol. 28, no. 2, 100–107
doi: 10.1093/glycob/cwx100
Advance Access Publication Date: 26 December 2017
Original Article

Microbial Biology

Interaction of *Neisseria meningitidis* Group X *N*-acetylglucosamine-1-phosphotransferase with its donor substrate

Shonoi A Ming[2], Ebony Cottman-Thomas[2], Natalee C Black[2], Yi Chen[3], Vamsee Veeramachineni[2], Dwight C Peterson[2], Xi Chen[3], Lauren M Tedaldi[4], Gerd K Wagner[4], Chao Cai[5], Robert J Linhardt[5], and Willie F Vann[2,1]

[2]Laboratory of Bacterial Polysaccharides, FDA, Silver Spring, MD 20993, USA, [3]Department of Chemistry, University of California, Davis, CA 95616, USA, [4]Department of Chemistry, King's College, London SE 11DB, UK, and [5]Department of Chemistry and Chemical Biology, Rensselaer Polytechnic Institute, Troy, NY 12180, USA

[1]To whom correspondence should be addressed: Tel: +1-240-402-7438; e-mail: willie.vann@fda.hhs.gov

Received 29 September 2017; Revised 21 November 2017; Editorial decision 1 December 2017; Accepted 5 December 2017

Abstract

Neisseria meningitidis Group X is an emerging cause of bacterial meningitis in Sub-Saharan Africa. The capsular polysaccharide of Group X is a homopolymer of *N*-acetylglucosamine α(1–4) phosphate and is a vaccine target for prevention of disease associated with this meningococcal serogroup. We have demonstrated previously that the formation of the polymer is catalyzed by a phosphotransferase which transfers *N*-acetylglucosamine-1-phosphate from UDP-*N*-acetylglucosamine to the 4-hydroxyl of the *N*-acetylglucosamine on the nonreducing end of the growing chain. In this study, we use substrate analogs of UDP-GlcNAc to define the enzyme/donor substrate interactions critical for catalysis. Our kinetic analysis of the phosphotransferase reaction is consistent with a sequential mechanism of substrate addition and product release. The use of novel uracil modified analogs designed by Wagner et al. enabled us to assess whether the CsxA-catalyzed reaction is consistent with a donor dependent conformational change. As expected with this model for glycosyltransferases, UDP-GlcNAc analogs with bulky uracil modifications are not substrates but are inhibitors. An analog with a smaller iodo uracil substitution is a substrate and a less potent inhibitor. Moreover, our survey of analogs with modifications on the *N*-acetylglucosamine residue of the sugar nucleotide donor highlights the importance of substituents at C2 and C4 of the sugar residue. The hydroxyl group at C4 and the structure of the acyl group at C2 are very important for specificity and substrate interactions during the polymerization reaction. While most analogs modified at C2 were inhibitors, acetamido analogs were also substrates suggesting the importance of the carbonyl group.

Key words: capsular polysaccharide, GlcNAc phosphotransferase, UDP-GlcNAc analogs

Introduction

Neisseria meningitidis, like many pathogenic bacteria, is encapsulated with serotype-specific acidic polysaccharides. These polysaccharides act as virulence factors by providing a shield against the host immune system. Capsular polysaccharides are important to the public health as convenient targets for vaccine development. *Neisseria meningitidis* is a major cause of bacterial meningitis worldwide resulting in significant numbers of deaths and morbidity

annually. Of the 12 polysaccharide-based serogroups of *N. meningitidis*, groups A, B, C, W-135, X and Y cause most of the meningococcal disease. Until recently, most of the epidemics of meningococcal disease in the meningitis belt of sub-Saharan Africa were caused by *N. meningitidis* group A. Recently, a glycoconjugate vaccine developed against group A, MenAfriVac was introduced in sub-Saharan Africa. The introduction of this vaccine has resulted in group A related disease being dramatically reduced to a few cases in vaccinated populations (Daugla et al. 2013). However, meningococcal group X associated disease has increased in recent years and is thus a target for vaccine development (Xie et al. 2013).

The *N. meningitidis* groups A and X capsular polysaccharides are homopolymers of phosphodiester linked *N*-acetylhexosamine-1-phosphate. The gene cluster encoding the NmX polysaccharide biosynthesis was first described in detail by Swartley et al. (1998). The gene cluster is organized similar to polysaccharide pathways that use an ABC transporter mechanism (Whitfield and Roberts 1999), containing two ABC transporter genes, and a region specific to synthesis of the polysaccharide structure. The genes specific for synthesis of NmX polysaccharide consist of *csxABC* (previously *xcbABC*). Muindi et al. (2014) and Fiebig et al. (2014) have shown that the *csx*A gene encodes an *N*-acetylglucosamine-1-phosphotransferase responsible for elongation of the growing polysaccharide chain of α(1–4)*N*-acetylglucosamine phosphate. The enzyme transfers GlcNAc-1-P from UDP-GlcNAc to the 4-hydroxyl of the nonreducing terminal GlcNAc on the growing chain. It thus belongs to a group of carbohydrate utilizing phosphotransferases primarily involved in microbial polysaccharide biosynthesis. These enzymes transfer sugar-1-phosphate from sugar nucleotide diphosphate to an acceptor without involving the anomeric center (Scheme 1). The catalytic subunit of lysosomal *N*-acetylglucosamine-1-phosphotransferase in the mannose–phosphate pathway has homology with CsxA (Muindi et al. 2014) and similarly catalyzes the transfer of GlcNAc-1-P to protein bound mannose. The catalytic mechanism of this group of enzymes has not been defined and structural data are lacking.

Understanding the mechanism of the enzymes that form bacterial capsular polysaccharides could help facilitate the development of drugs that inhibit polysaccharide formation and thereby provide an additional tool for the control of the disease caused by encapsulated pathogens. In our previous work, we showed that the minimum acceptor for the *CsxA* is a trimer (Muindi et al. 2014). Here we have used substrate analogs to explore the interaction of CsxA with its donor substrate UDP-GlcNAc. In this report, we show that substitution of the uracil with bulky groups can inhibit turnover. In addition, our results help to define sites on the sugar portion of the UDP-GlcNAc donor that are important for the specificity of the enzyme in catalyzing polymerization reactions.

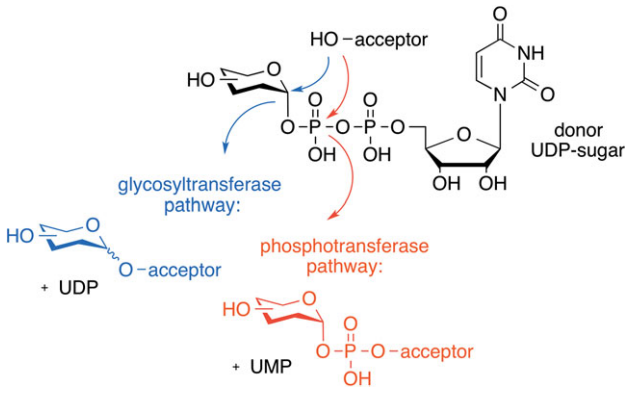

Scheme 1.

Results and Discussion

Bacterial capsular polysaccharides are often composed of phosphodiester linked monosaccharides. The phosphodiester linked monosaccharide units in these polysaccharides are added by transfer from a sugar nucleotide substrate. This is analogous to addition of glycoside units by glycosyltransferases (Scheme 1). While the bonds formed in these two cases are quite distinct, structural similarities that are related to the interaction of the sugar nucleotides substrate have been observed between glycosyltransferases and other enzymes that use nucleotide sugars (Campbell et al. 2000). Glycosyltransferases that form polysaccharides and oligosaccharides are well studied, while bacterial phosphotransferases that form phosphodiester linked polysaccharides are not. In this report, we explore the interaction of a bacterial phosphotransferase with its donor substrate.

N-Acetylhexosamine-1-phosphotransferases use the same sugar nucleotide donors as glycosyltransferases that catalyze the transfer of the corresponding *N*-acetylhexosamine. Many glycosyltransferases catalyze the transfer of the sugar to the acceptor substrate via an ordered sequential mechanism, where the sugar nucleotide donor binds first. Kinetic characterization of *N*-acetylhexosamine-1-phosphotrasferases is limited. As a first step to understanding how these enzymes interact with their substrates, we determined the steady-state kinetic parameters of *CsxA*.

CsxA mechanism of action

We have determined k_{cat} and K_m for both the donor substrate UDP-GlcNAc and the acceptor substrate, NmX polysaccharide. The NmX polysaccharide acceptor had an average size of 235 repeat units of GlcNAc-1-phosphate. The polysaccharide was dephosphorylated at the nonreducing end prior to use as an acceptor. In Figure 1A, K_m and k_{cat} values were determined for the acceptor at a saturating concentration of the donor substrate UDP-GlcNAc. The nonlinear least squares fit of the data to the Michaelis–Menten equation gave values of $k_{cat} = 74.6 \pm 3.3\ min^{-1}$ and $K_m = 0.20 \pm 0.04\ \mu M$. We note that a K_m in the nanomolar range highlights the high affinity of CsxA for the NmX polysaccharide. In a similar fashion, the k_{cat} and K_m values were determined for UDP-GlcNAc at a saturating concentration of the acceptor substrate NmX polysaccharide. The data in Figure 1B were fit to the Michaelis–Menten equation and gave values of $k_{cat} = 84.9 \pm 4.5\ min^{-1}$ and $K_m = 46.5 \pm 7.4\ \mu M$. The K_m for UDP-GlcNAc is similar to values reported for *N*-acetylhexosaminyl transferases.

We further explored the steady-state kinetic mechanism by generating double reciprocal plots of initial velocity vs. substrate concentration. In Figure 2A, the reaction was followed at varying concentrations of UDP-GlcNAc at several fixed concentrations of NmX polysaccharides and vice versa in Figure 2B. The plots yield a series of intersecting lines indicative of a multisubstrate enzyme reaction proceeding via a sequential mechanism in which the substrates bind to the enzyme in a sequential fashion prior to the dissociation of the first product. This finding is in agreement with prior studies of glycosyltransferases where the glycosylation reaction follows a sequential bi–bi mechanism (Liang et al. 2015). In this mechanism, the sugar donor and the acceptor are bound sequentially followed by transfer of the sugar moiety from donor to acceptor. At the completion of the reaction, the glycosylated

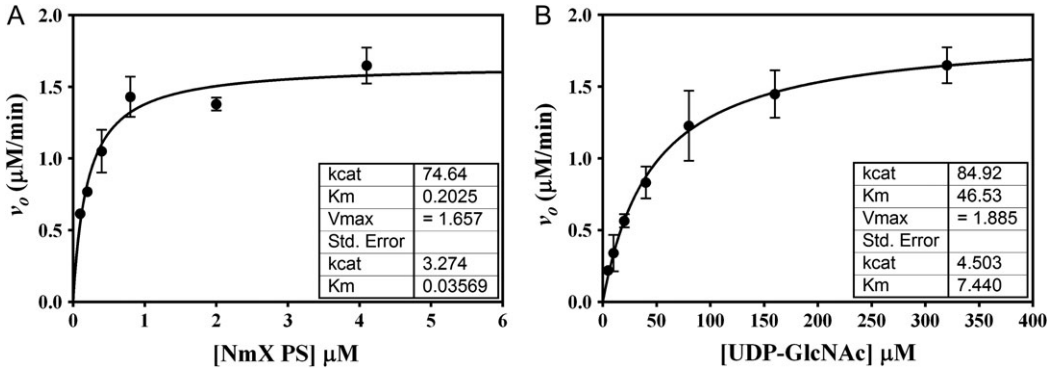

Fig. 1. The dependence of v_o (μM/min) for the transfer of GlcNAc-1-phosphate from UDP-GlcNAc to NmX polysaccharide catalyzed by CsxA (22 nM). (A) NmX polysaccharide concentration was varied from 0.1 to 4.1 μM with a fixed concentration of UDP-GlcNAc at 320 μM. (B) UDP-GlcNAc concentration was varied from 5 to 320 μM with a fixed concentration of NmX polysaccharide at 4.1 μM. The nonlinear least squares fit of the data were fitted to the Michaelis–Menten kinetics equation.

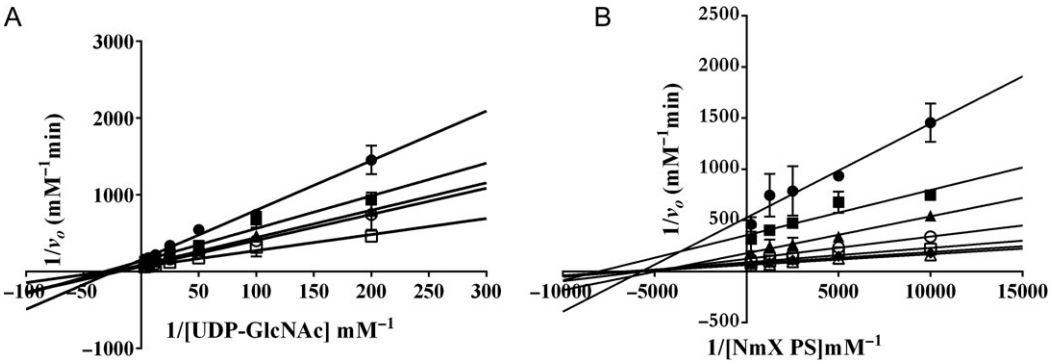

Fig. 2. Initial velocity data are presented in the form of double reciprocal plots of 1/velocity vs. 1/[substrate]. (A) UDP-GlcNAc concentration was varied from 5 to 320 μM while holding the NmX polysaccharide concentration constant at: (●) 0.1 μM, (■) 0.2 μM, (▲) 0.4 μM, (○) 0.8 μM, (□) 4.1 μM. (B) NmX polysaccharide concentration was varied from 0.1 to 4.1 μM while holding the UDP-GlcNAc concentration constant at: (●) 5 μM, (■) 10 μM, (▲) 20 μM, (○) 40 μM, (□) 80 μM (♦) 160 μM or (Δ) 320 μM.

product is released followed by the release of the nucleotide moiety. An ordered sequential mechanism has also been proposed for the non-glycosyltransferase TagF (Sewell et al. 2009). TagF is also a polymerizing phosphotransferase that catalyzes the formation of the glycerol teichoic acid in *Bacillus subtilis* 168 by the transfer of glycerol phosphate from CDP-glycerol to a hydroxyl of glycerol at the end of the growing teichoic acid chain.

Effect of modifications at UDP-GlcNAc's uracil moiety

The fact that the nucleotide sugar was required to bind prior to the acceptor in several glycosyltransferases led Qasba et al. (2005) to postulate a donor-induced conformational change. He postulated based on crystallographic data that the initial binding of the nucleotide donor result in a conformational change of an internal loop facilitating subsequent acceptor binding. Wagner developed a series of broad-spectrum glycosyltransferase inhibitors targeting this mechanism (Jorgensen et al. 2013). This class of glycosyltransferase inhibitors is characterized by a bulky substituent at position 5 of the uracil moiety of the UDP-sugar donor, which interferes with the movement of this loop during the glycosyltransferase catalytic mechanism.

We tested CsxA to determine whether the polymerization reaction was similarly inhibited by this group of UDP-GlcNAc analogs (Table I). The three UDP-GlcNAc analogs examined were modified at the C5 position of the uracil moiety with either a bulky 5-formylthien-2-yl or 5-carboxythien-2-yl group, or a smaller iodine. All of these analogs inhibited catalytic activity. However, only the analog with an iodine substituent at C5 was found to be a substrate for CsxA (Figure 3) and resulted in the formation of oligosaccharides. It is important to note that this analog had the smallest modification at C5 of the uracil. It has been shown by Jorgensen et al. (2013) that the standard catalytic pathway of a blood-group glycosyltransferase can be disrupted by introduction of bulky substituents at the C5 position of the UDP-sugar donor. They propose that this disruption is due to the bulky substituent preventing the proper orientation of an active site loop critical for substrate binding and thus catalysis. While we do not have structural data to support the presence of an analogous loop in CsxA, one could explain the observation by interference with an important conformational change by the bulk substituents on the uracil. Definitive proof of such interference awaits the results crystallographic data on CsxA.

Specificity of CsxA for sugar moiety

We compared the kinetic parameters for the natural substrate UDP-GlcNAc and a variety of substrate analogs to determine the sugar substrate specificity of CsxA (Table II). We initially explored commercially available UDP-GalNAc and UDP-Glc as substrates and

Table I. Percent inhibition of CsxA reaction by uracil modified donors

Inhibitors		5 mM (%)	1 mM (%)	0.1 mM (%)
1A	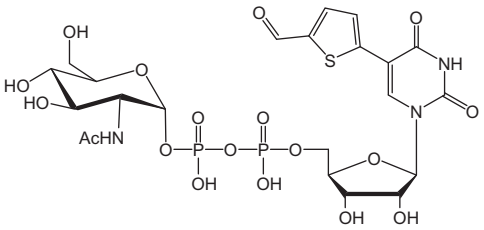	98	52	36
1B	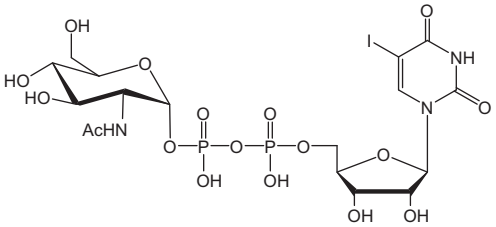	78	45	33
1C	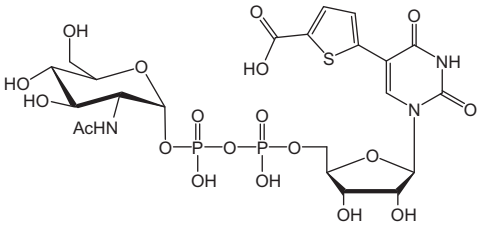	100	79	43

Percent inhibition of the CsxA activity using varying concentrations of uracil modified UDP-GlcNAc as inhibitors. Values were obtained using radiolabeled paper chromatography assay after a 1 h incubation at 37°C.

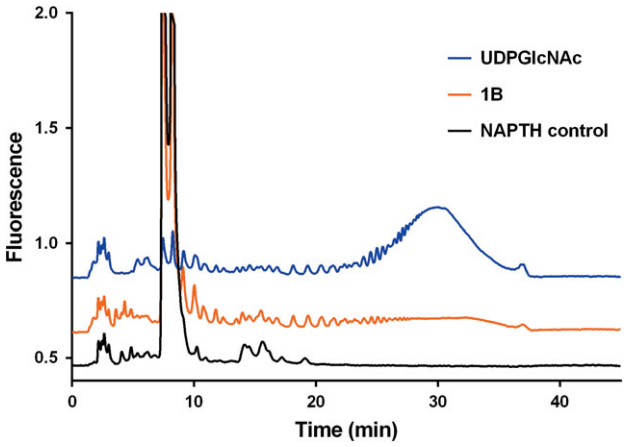

Fig. 3. CsxA-catalyzed elongation of the capsular polysaccharide chain using uracil modified UDP-GlcNAc analog 1B (100 μM) as the donor substrate. Total incubation time = 4 h.

found that the CsxA did not utilize either as a substrate, nor were either of them found to be inhibitors. This finding highlights the importance of the interactions made between the CsxA catalytic site and the *N*-acetyl group at C2 and the hydroxyl group at C4.

We synthesized UDP-4-fluoro-*N*-acetylglucosamine (UDP-4F-GlcNAc) to further investigate the role of the substituent at C4 using a chemoenzymatic approach. 4-Deoxy-4-fluoro-*N*-acetylglucosamine (4F-GlcNAc) was prepared from *N*-acetylgalactosamine (GalNAc) using a modification of the synthetic route previously described (Zhai et al. 2012). Reaction of the axial four hydroxyl of GalNAc, with diethylamino sulfur trifluoride installed the C4 fluoride functionality with an equatorial configuration. UDP-4F-GlcNAc was prepared from 4F-GlcNAc enzymatically using enzymes NahK and GlmU. NahK, an *N*-acetylhexosamine 1-phosphate kinase from *Bifidobacterium longum* was found to be quiet promiscuous to various GlcNAc 3- and 4-epimers (Cai et al. 2009). This combined with the previously known use of *Escherichia coli* GlmU with 4F-GlcNAc as a substrate (Schultz et al. 2017) helped us in the design of a single pot reaction to directly synthesize UDP-4F-GlcNAc from 4F-GlcNAc in high yields. The analog UDP-4-fluoro-*N*-acetylglucosamine is a substrate and adds a single residue to the fluorescent oligosaccharide acceptor, but turns over at a fraction of the rate of the native substrate UDP-GlcNAc (Figure 4). This slow rate of turnover suggests that the equatorial 4-hydroxyl may, in addition to being the reactive moiety on the acceptor, play another role in substrate interaction with the enzyme and donor specificity. A similar specificity pattern was observed with the *E. coli N*-acetylglucosaminyltransferase MurG, an enzyme in the pathway for peptidoglycan biosynthesis. No inhibition of MurG was observed with UDP-GalNAc, nor was the sugar nucleotide active as a substrate (Ha et al. 1999). A crystal structure of MurG with the donor substrate UDP-GlcNAc revealed interactions between the 4-hydroxyl and essential amino acid side chains that would not be accessible to the axial 4-hydroxyl of UDP-GalNAc (Hu et al. 2003).

Effect of modifications at UDP-GlcNAc's C2 position on catalysis

We studied the kinetic properties of CsxA toward a variety of UDP-GlcNAc analogs modified at the C2 or C6 carbons (Table II) or on the *N*-acyl functional group to further investigate the substrate specificity for the sugar residue. All of the analogs were inhibitors, with the best inhibitor being the analogs with modified acyl groups (2D and 2E).

Table II. Percent inhibition of CsxA reaction by donors with modified sugar

Inhibitors		0.3 mM (%)	0.1 mM (%)
2A	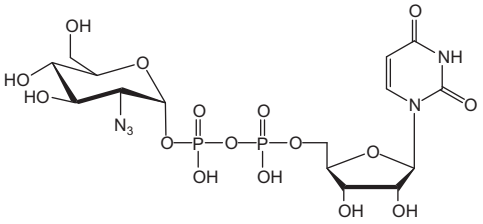	86	78
2B	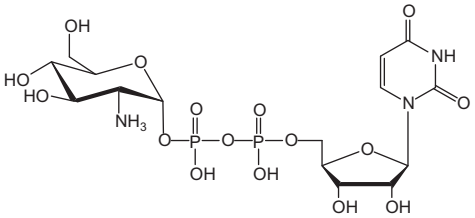	80	53
2C	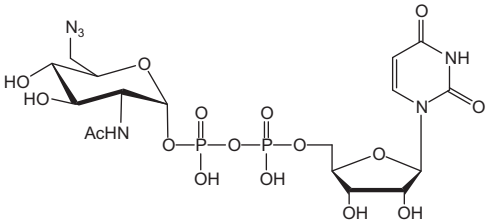	47	41
2D	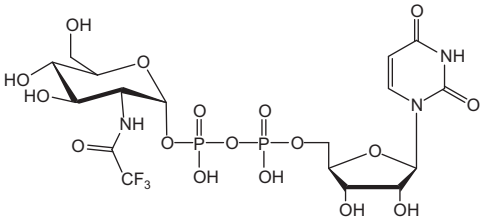	93	84
2E	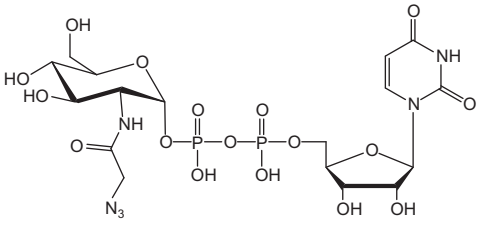	98	89

Percent inhibition of the CsxA activity using varying concentrations of sugar modified UDP-GlcNAc as inhibitors. Values were obtained using radiolabeled paper chromatography assay after a 1 h incubation at 37°C.

Interestingly the UDP-glucosamine was a less effective inhibitor than UDP-2-azidoglucose. All of the analogs tested served as donor substrates for CsxA as indicated by addition to the fluorescent tetrasaccharide detected by the HPLC assay (Figure 5). However, not all of the analogs were readily converted to higher MW oligosaccharides. The sugar modified analogs UDP-GlcNFTA (2D) and UDP-GlcNAz (2E) were found to be the best substrates of those tested, suggesting the importance of the acyl group. Compound 2D is a weak substrate that is converted to product at a much slower apparent rate than UDP-GlcNAc (Figure 5). Note that all of the starting material is consumed when 2D and UDP-GlcNAc are incubated with CsxA for 4 h. At much shorter periods of time (data not shown) only UDP-GlcNAc is rapidly consumed under similar conditions and 2D results in the formation of smaller intermediates. We further characterized these substrate analogs kinetically using a coupled assay to measure UMP production. Although all of the analogs were turned over by CsxA, the rate of turnover was 80% slower and with a K_m value increase of up to 90% more than that observed with UDP-GlcNAc (Table III). These large effects on k_{cat} and K_m led to an overall decrease in the catalytic efficiency of up to 98% for CsxA. The K_m for the UDP-GlcNFTA and UDP-GlcNAz increased 5- and 10-fold, respectively, over the natural substrate suggesting that the changes in the structure of the acyl side chain has a significant effect on donor substrate binding.

Summary

The CsxA of *N. meningitidis* group X catalyzes polymerization of *N*-acetylglucosamine-1-P through a sequential mechanism as has

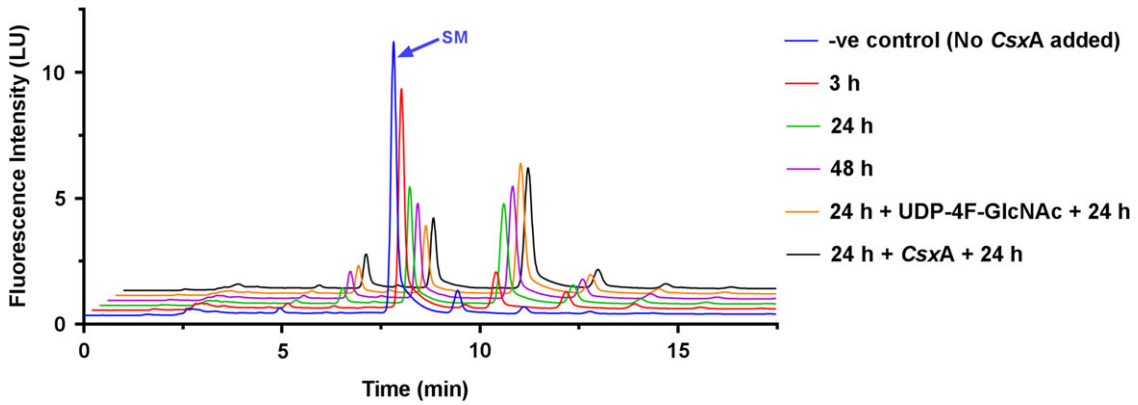

Fig. 4. *Csx*A (2.25 μM) catalyzed elongation of napthalimide-labeled NmX tetrasaccharide (1 μM) using UDP-4F-GlcNAc (66.6 μM) as the donor substrate. After the respective incubation times (as reported in the figure) the reactions were stopped or spiked in with a second equivalent dose of UDP-4F-GlcNAc and *Csx*A.

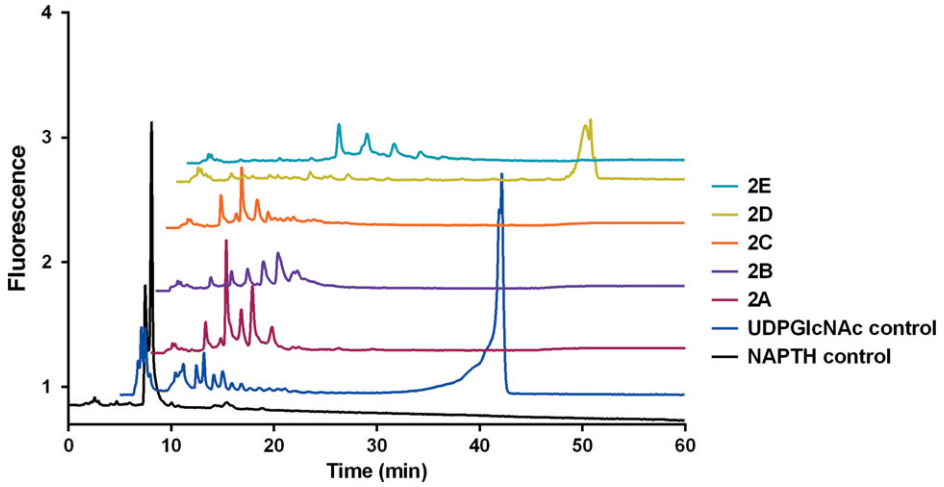

Fig. 5. CsxA-catalyzed elongation of the capsular polysaccharide chain using UDP-GlcNAc analogs containing sugar modifications (300 μM) as the donor substrates. Total incubation time = 4 h.

Table III. Kinetic parameters of CsxA for donors with acyl modified sugars

Substrate	k_{cat} (min^{-1})	K_m (μM)	k_{cat}/K_m (μM/min)
UDP-GlcNAc	10.6 ± 0.2	21.1 ± 2.4	0.50 ± 0.07
UDP-NFTA	2.3 ± 0.3	212.1 ± 67.5	0.01 ± 0.004
UDP-NAz	1.5 ± 0.2	98.8 ± 38.0	0.01 ± 0.005

Kinetic parameters determined from the nonlinear least squares fit of v_o vs. substrate concentration at a constant concentration of 100 μg/mL hydrolyzed NmX polysaccharide to the Michaelis–Menten equation.

been described for many glycosyltransferases. We have used substrate analogs to define the specificity of interactions with the enzyme and the nucleotide donor. Based on the results from the analogs available to us we can conclude that the hydroxyl group at C4 and the structure of the acyl group at C2 are very important for specificity and substrate interactions during the polymerization reaction. We have also described a chemoenzymatic route to the chain terminating substrate UDP-4F-GlcNAc.

Materials and Methods

Synthesis of UDP-GlcNAc analogs

The UDP-GlcNAc analogs were synthesized as previously reported with the exception of UDP-4F-GlcNAc (synthesis reported in Supplementary data) (Chen et al. 2011; Tedaldi et al. 2012).

Bacterial strains and plasmids

The bacterial strains and pWM300 expression plasmid used in this study has been previously described (Muindi et al. 2014).

Expression and purification of CsxA

The plasmid, pWM300, for expressing the CsxA gene, was transformed into *E. coli* BL21(DE3)STAR™ cells (Invitrogen, C6010-03). A starter culture containing 32 mL LB Broth, Lennox supplemented with 0.05% glucose (Sigma, G8270) and 100 μg/mL ampicillin (Fisher Scientific, BP1760-25) was inoculated with a single colony from the freshly transformed *E. coli* BL21(DE3)STAR™ cells. The culture was grown at 37°C with shaking at 270 rpm until absorbance at 600 nm of 0.5–1.0. This starter culture was used to inoculate 500 mL ZYP-5052

rich medium for auto-induction (Studier 2014) with shaking at 110 rpm for 18 h at 30°C. The cells are harvested by centrifugation and resuspended in 20 mL of 50 mM Tris–HCl, 25 mM $MgCl_2$, pH 8.0, supplemented with 3.5 mL of protease inhibitor cocktail (Sigma, P8465). The resuspended cells were lysed by passage through a chilled French Press cell and the cellular debris was removed by centrifugation at 10,000 × *g* for 15 min. The membrane fragments were removed from the cytosol by ultracentrifugation at 100,000 × *g* for 1 h. The cytosolic fraction was purified on a BioRad NGC FPLC equipped with a 5 mL HisTrap HP Column (GE Healthcare, 17-5248-02). The column was washed with 50 mM Tris–HCl, 0.1 M NaCl, pH 8.0, followed by 50 mM Tris–HCl, 0.1 M NaCl, 25 mM imidazole, 50 mM imidazole and 100 mM imidazole, pH 8.0, respectively, until protein was not detected in the fractions by Bradford assay. CsxA was eluted with 50 mM Tris–HCl, 0.1 M NaCl, 250 mM imidazole, pH 8.0. The elution fractions with the highest absorbance were pooled and concentrated using Amicon Ultra Centrifuge Devices 10 K MW cutoff (Sigma, UFC801024). The pooled fraction was analyzed by SDS PAGE. CsxA enzymatic activity was assayed using paper chromatography assay, as previously described (Muindi et al. 2014). The purified CsxA sample was adjusted to 10% glycerol and stored at −80°C.

Preparation of acceptor substrates

Unlabeled dephosphorylated NMX polysaccharide: The phosphate residues on the nonreducing end of NmX polysaccharide were removed by bovine intestinal mucosal alkaline phosphatase (Sigma, P0114) in 5 mM Tris–HCl, 5 mM $MgCl_2$, 0.4 mM $ZnCl_2$, pH 8, incubated at 37°C for 4 h. The incubation mixture was then boiled for 1 min to denature the phosphatase, centrifuged and supernatant was dried overnight in a SpeedVac. The dephosphorylated polysaccharide was dissolved in H_2O and its average molecular weight was determined by light scattering.

Napthalimide-labeled NmX tetrasaccharide: NmX polysaccharide was mildly hydrolyzed with 1% acetic acid for 1 h at 80°C. The hydrolysate was dried overnight on a SpeedVac. An azide group was added to the terminal *N*-acetylglucosamine by dissolving the hydrolysate in H_2O and incubating it at 4°C for 18 h with 162 mM 2-chloro-1,3-dimethylimidazolinium chloride (Sigma, 529,249), 580 mM NaN_3 and 636 mM 2,6-lutidine. The reaction mixture was desalted on a Biogel P2 column. The fractions containing the azide modified NmX oligosaccharides were identified. The pooled oligosaccharide fractions were converted to the fluorescent naphthalimide modification by adding 625 µM of 4-ethynyl-*N*-ethyl-1,8-naphthalimide dye and click reagents (Mosley et al. 2010) with incubation for 1 h at 37°C. Fluorescent oligosaccharides were desalted on Biogel P2 and the pooled fractions evaporated to dryness.

The oligosaccharides were dephosphorylated as described above and loaded onto a C18 Sep-Pak (Waters, 051,910) and eluted with 50% acetonitrile to desalt.

The dephosphorylated naphthalimide oligosaccharides were further purified on Silica Gel 60 TLC plates (Whatman) with a 6:2:4:2 ethyl acetate:acetic acid:methanol:water solvent system. Oligosaccharides were recovered from the silica with water, passed through C18 Sep-Pak and eluted with 50% acetonitrile. The oligosaccharides were analyzed by MALDI-MS using saturated 6-aza-2-thiothymine in 20% acetonitrile as the matrix.

Determination CsxA enzymatic activity using paper chromatography

The purified CsxA enzymatic activity was determined by radiolabeled chromatography assay (Muindi et al. 2014).

Determination CsxA enzymatic activity using a multienzyme coupled assay

This multienzyme assay couples CsxA activity to the disappearance of NADH at 340 nm as previously described (Gosselin et al. 1994; Freiberger et al. 2007; Muindi et al. 2014) with some minor modifications. The assays were performed in quartz cuvettes and monitored with a Jasco Inc., dual beam UV–Vis spectrophotometer equipped with an air Peltier temperature system. The reactions in a total volume of 200 µL were conducted at 25°C in 50 mM HEPES, 25 mM $MgCl_2$, 0.1 M NaCl, pH 7.4. The reference and the sample cuvettes contained the following; 2.7–5.4 µM, unlabeled dephosphorylated *Nm*X capsular polysaccharide, 7 mM phosphoenolpyruvate, 2 mM ATP, 0.3 mM NADH, 320 µM UDP-GlcNAc, 0.2 U/mL NMPK, 12 U PK/LDH. Samples were allowed to incubate for 5 min at 25°C prior to initiating the reaction. Reactions were initiated by the addition of CsxA (20–70 nM) to the sample cuvette.

Determination of kinetic parameters

k_{cat} and K_m determined with natural substrates: The kinetic parameters for CsxA were determined using the multienzyme coupled assay described above. Reactions contained 5–320 µM UDP-GlcNAc, 0.1–4.0 µM unlabeled dephosphorylated *Nm*X capsular polysaccharide and initiated by the addition of CsxA (20–70 nM). Initial velocities were determined at varied donor concentrations, while holding the acceptor concentration constant at 4.0 µM. Similarly, initial velocities were determined at varied acceptor concentrations, while holding donor concentration constant at 320 µM. Apparent k_{cat} and K_m values were obtained by fitting the observed initial velocities to the Michaelis–Menten equation.

k_{cat} and K_m determined with UDP-GlcNAc substrate analogs: Using the multienzyme coupled assay, the apparent k_{cat} and K_m values were determined for the UDP-GlcNAc substrate analogs, UDP-GlcNTFA and UDP-GlcNAz. The concentration of the unlabeled dephosphorylated *Nm*X capsular oligosaccharide acceptor was held constant at 100 µg/mL while the concentration of UDP-GlcNAc analogs was varied (38–500 µM).

Substrate/inhibitor screen of UDP-GlcNAc analogs

Initial inhibitor screens of the UDP-GlcNAc analogs were performed using the radiolabeled paper chromatography assay described above. Specifically, inhibitor concentrations ranging from 0.1 to 5 mM were incubated with 50 µM UDP-N-acetyl [^{14}C] D-glucosamine (specific activity 55 mCi/mmol) (American Radiolabelled Chemicals, Saint Louis, MO), 2 µg unlabeled NmX polysaccharide, in 50 mM Tris, 25 mM $MgCl_2$, pH 8, for 1 h at 37°C in a total reaction volume of 50 µL. In addition, the multienzyme coupled assay described above was also used to further screen the UDP-GlcNAc analogs as substrates and/or inhibitors for CsxA. In this case, the reactions to determine if an analog was a substrate contained 100 µg/mL unlabeled dephosphorylated NmX capsular oligosaccharide acceptor and 300 µM of the analog and were initiated by the addition of 69 nM of CsxA to the sample cuvette and monitored for 1 h. The reactions contained 300 µM of the analog and 50 µM of the natural substrate, UDP-GlcNAc to screen analogs for inhibitory activity. The reactions were initiated by the addition of 69 nM of CsxA to sample cuvette and monitored for 1 h.

HPLC analysis of fluorescent oligosaccharide elongation

Reactions are performed in 50 mM HEPES, 25 mM $MgCl_2$, 0.1 M NaCl pH 7.4 with a total reaction volume of 10 or 50 µL. Each reaction mixture contained 50 µM or 1 mM UDP-GlcNAc, 0.1–5 mM UDP-GlcNAc sugar modified or uracil modified analog, 350 nM fluorescently

labeled oligosaccharide and 250–500 ng/mL CsxA and allowed to proceed for 1 h or 4 h at 37°C. The reactions are quenched by the addition of ethanol. The samples are subsequently freeze-dried and resuspended in 30 μL of H_2O prior to HPLC analysis. Oligosaccharides were separated by anion exchange chromatography on a DNA SWIFT™ SAX-1S monolith column (Thermo Scientific Dionex). HPLC analysis was carried out on an Agilent Technologies 1200 Series system with an in-line fluorescence detector.

Supplementary data

Supplementary data is available at *Glycobiology* online.

Funding

GKW thanks the Medical Research Council (MRC) for financial support (grant G0901746), and the Engineering and Physical Sciences Research Council (EPSRC) National Mass Spectrometry Facility, Swansea, for the recording of mass spectra.

Acknowledgements

We wish to thank Marcos Battistel for NMR analysis.

Conflict of interest statement

None declared.

References

Cai L, Guan W, Kitaoka M, Shen J, Xia C, Chen W, Wang PG. 2009. A chemoenzymatic route to N-acetylglucosamine-1-phosphate analogues: Substrate specificity investigations of N-acetylhexosamine 1-kinase. *Chem Commun (Camb)*. 2944–2946.

Campbell RE, Mosimann SC, Tanner ME, Strynadka NC. 2000. The structure of UDP-N-acetylglucosamine 2-epimerase reveals homology to phosphoglycosyl transferases. *Biochemistry*. 39:14993–15001.

Chen Y, Thon V, Li Y, Yu H, Ding L, Lau K, Qu J, Hie L, Chen X. 2011. One-pot three-enzyme synthesis of UDP-GlcNAc derivatives. *Chem Commun (Camb)*. 47:10815–10817.

Daugla DM, Gami JP, Gamougam K, Naibei N, Mbainadji L, Narbé M, Toralta J, Kodbesse B, Ngadoua C, Coldiron ME et al. 2013. Effect of a serogroup A meningococcal conjugate vaccine (PsA–TT) on serogroup A meningococcal meningitis and carriage in Chad: A community study. *Lancet*. 383:40–47.

Fiebig T, Berti F, Freiberger F, Pinto V, Claus H, Romano MR, Proietti D, Brogioni B, Stummeyer K, Berger M et al. 2014. Functional expression of the capsule polymerase of *Neisseria meningitidis* serogroup X: A new perspective for vaccine development. *Glycobiology*. 24:150–158.

Freiberger F, Claus H, Gunzel A, Oltmann-Norden I, Vionnet J, Muhlenhoff M, Vogel U, Vann WF, Gerardy-Schahn R, Stummeyer K. 2007. Biochemical characterization of a *Neisseria meningitidis* polysialyltransferase reveals novel functional motifs in bacterial sialyltransferases. *Mol Microbiol*. 65:1258–1275.

Gosselin S, Alhussaini M, Streiff MB, Takabayashi K, Palcic MM. 1994. A continuous spectrophotometric assay for glycosyltransferases. *Anal Biochem*. 220:92–97.

Ha S, Chang E, Lo MC, Men H, Park P, Ge M, Walker S. 1999. The kinetic characterization of *Escherichia coli* MurG using synthetic substrate analogues. *J Am Chem Soc*. 121:8415–8426.

Hu Y, Chen L, Ha S, Gross B, Falcone B, Walker D, Mokhtarzadeh M, Walker S. 2003. Crystal structure of the MurG:UDP-GlcNAc complex reveals common structural principles of a superfamily of glycosyltransferases. *Proc Natl Acad Sci USA*. 100:845–849.

Jorgensen R, Pesnot T, Lee HJ, Palcic MM, Wagner GK. 2013. Base-modified donor analogues reveal novel dynamic features of a glycosyltransferase. *J Biol Chem*. 288:26201–26208.

Liang DM, Liu JH, Wu H, Wang BB, Zhu HJ, Qiao JJ. 2015. Glycosyltransferases: Mechanisms and applications in natural product development. *Chem Soc Rev*. 44:8350–8374.

Mosley SL, Rancy PC, Peterson DC, Vionnet J, Saksena R, Vann WF. 2010. Chemoenzymatic synthesis of conjugatable oligosialic acids. *Biocatal Biotransform*. 28:41–50.

Muindi KM, McCarthy PC, Wang T, Vionnet J, Battistel M, Jankowska E, Vann WF. 2014. Characterization of the meningococcal serogroup X capsule N-acetylglucosamine-1-phosphotransferase. *Glycobiology*. 24:139–149.

Qasba PK, Ramakrishnan B, Boeggeman E. 2005. Substrate-induced conformational changes in glycosyltransferases. *Trends Biochem Sci*. 30: 53–62.

Schultz VL, Zhang X, Linkens K, Rimel J, Green DE, DeAngelis PL, Linhardt RJ. 2017. Chemoenzymatic synthesis of 4-fluoro-N-acetylhexosamine uridine diphosphate donors: Chain terminators in glycosaminoglycan synthesis. *J Org Chem*. 82:2243–2248.

Sewell EW, Pereira MP, Brown ED. 2009. The wall teichoic acid polymerase TagF is non-processive in vitro and amenable to study using steady state kinetic analysis. *J Biol Chem*. 284:21132–21138.

Studier FW. 2014. Stable expression clones and auto-induction for protein production in *E. coli*. *Methods Mol Biol*. 1091:17–32.

Swartley JS, Liu LJ, Miller YK, Martin LE, Edupuganti S, Stephens DS. 1998. Characterization of the gene cassette required for biosynthesis of the (alpha1–>6)-linked N-acetyl-D-mannosamine-1-phosphate capsule of serogroup A *Neisseria meningitidis*. *J Bacteriol*. 180:1533–1539.

Tedaldi LM, Pierce M, Wagner GK. 2012. Optimised chemical synthesis of 5-substituted UDP-sugars and their evaluation as glycosyltransferase inhibitors. *Carbohydr Res*. 364:22–27.

Whitfield C, Roberts IS. 1999. Structure, assembly and regulation of expression of capsules in *Escherichia coli*. *Mol Microbiol*. 31:1307–1319.

Xie O, Pollard AJ, Mueller JE, Norheim G. 2013. Emergence of serogroup X meningococcal disease in Africa: Need for a vaccine. *Vaccine*. 31: 2852–2861.

Zhai Y, Liang M, Fang J, Wang X, Guan W, Liu XW, Wang P, Wang F. 2012. NahK/GlmU fusion enzyme: Characterization and one-step enzymatic synthesis of UDP-N-acetylglucosamine. *Biotechnol Lett*. 34:1321–1326.